New Journal of Physics
The open-access journal for physics

The nature of the low-energy excitations in the short-range-ordered region of Cs_2CuCl_4 as revealed by ^{133}Cs nuclear magnetic resonance

M-A Vachon[1], G Koutroulakis[1], V F Mitrović[1,5], Ookie Ma[1], J B Marston[1], A P Reyes[2], P Kuhns[2], R Coldea[3] and Z Tylczynski[4]

[1] Department of Physics, Brown University, Providence, RI 02912, USA
[2] National High Magnetic Field Laboratory, Tallahassee, FL 32310, USA
[3] Clarendon Laboratory, Physics Department, University of Oxford, Parks Road, Oxford OX1 3PU, UK
[4] Institute of Physics, Adam Mickiewicz University, Umultowska 85, 61-614 Poznan, Poland
E-mail: vemi@brown.edu

New Journal of Physics **13** (2011) 093029 (13pp)
Received 8 April 2011
Published 19 September 2011
Online at http://www.njp.org/
doi:10.1088/1367-2630/13/9/093029

Abstract. We report nuclear magnetic resonance (NMR) measurements of the spin-1/2 anisotropic triangular lattice antiferromagnet Cs_2CuCl_4 as a function of temperature and applied magnetic field. The observed temperature and magnetic field dependence of the NMR relaxation rate suggests that low-energy excitations in the short-range-ordered region stabilized over a wide range of intermediate fields and temperatures of the phase diagram (sketched in figure 1(a)) are gapless or nearly gapless fermionic excitations. An upper bound on the size of the gap of 0.037 meV $\approx J/10$ is established. The magnetization and NMR relaxation rate can be qualitatively described either by a quasi-1D picture of weakly coupled chains or by mean-field theories of specific 2D spin liquids; however, quantitative differences exist between data and theory in both cases. This comparison indicates that 2D interactions are quantitatively important in describing the low-energy physics.

[5] Author to whom any correspondence should be addressed.

Contents

1. Introduction

The emergence of particles with fractional quantum numbers is among the most remarkable phenomena that may arise in strongly correlated electron systems. In one spatial dimension, the exact Bethe ansatz solution of the spin-1/2 Heisenberg antiferromagnetic chain provides a prototype, as the solution exhibits a non-magnetic spin liquid ground state with deconfined spin-1/2 (spinon) excitations [1, 2]. These excitations carry half of the local spin degree of freedom $\Delta S = \pm 1$. The existence of spinons as fractional elementary excitations has also been well established experimentally in quasi-1D antiferromagnets (AFs) [3].

The search for examples of spin fractionalization has turned to dimensions greater than one. Inelastic neutron scattering measurements on the 2D frustrated quantum AF Cs_2CuCl_4 with spins on an anisotropic triangular lattice have shown dominant continua of excitations as characteristic of spin-1/2 spinon quasi-particles [4, 5] and this has stimulated intense theoretical work to explain these findings [6–12]. Cs_2CuCl_4 is a hard insulator with orthorhombic space group where magnetic spin-1/2 Cu atoms form a linear chain, with coupling $J = 0.375$ meV, in the $\hat{b}$-direction. Chains are stacked together along the $\hat{c}$-axis separated by a distance of $b/2$ and with coupling $J' = 0.125$ meV [13, 14]. Thus, the spins form a frustrated anisotropic triangular lattice, as illustrated in figure 1(b). A small interplane coupling $J'' = 0.017$ meV (a-axis) stabilizes the long-range spiral order below 0.62 K in the zero applied field [14]. The schematic phase diagram of Cs_2CuCl_4 is shown in figure 1(a). A small Dzyaloshinskii–Moriya (DM) interaction $D \sim 5\% J$ (which we neglect in the calculations presented below) is present along the interchain links. At intermediate temperatures ($T \approx 400$ mK to 2.5 K) a short-range-ordered (SRO) region is stabilized on application of a magnetic field ($\mathbf{H} = H\hat{z}$) of sufficient strength along any of the three crystalline axes [4, 5, 15]. The magnetic field breaks the full spin–rotational symmetry of an isotropic system, but the subgroup of U(1) rotations in the plane perpendicular to the field remains unbroken in the SRO region.

Kohno *et al* [11] have shown that many features of the experimental data in Cs_2CuCl_4 can be understood by viewing the anisotropic triangular lattice of spins as a system of weakly coupled 1D Heisenberg chains. The work has recently been extended to include the effects of an external magnetic field [12], but not yet nonzero temperatures. As our focus here is on the SRO regime at intermediate temperatures, we also compare the data to alternative relevant models of spin liquid states proposed previously for the 2D anisotropic triangular lattice, where

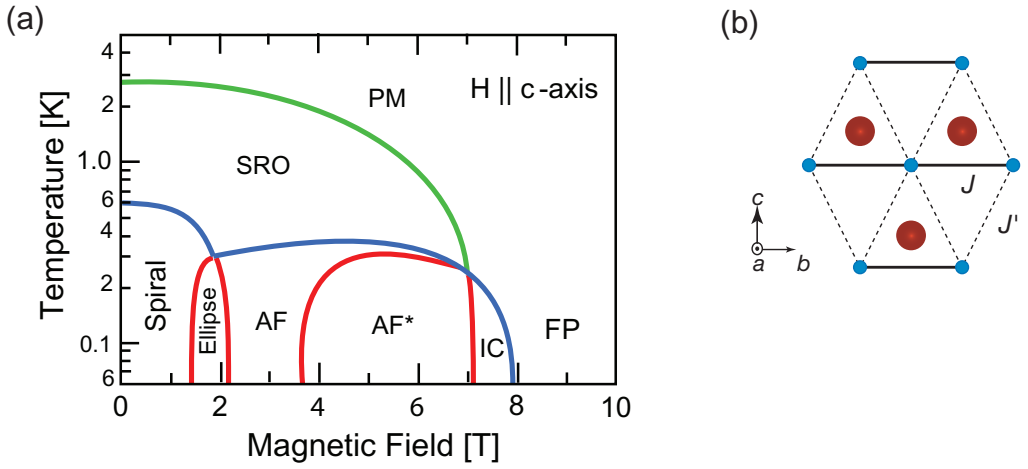

Figure 1. (a) Schematic phase diagram of Cs_2CuCl_4 for magnetic field applied along the $\hat{c}$-axis based on the results of [15, 16]. The green lines indicate the maximum in the temperature dependence of susceptibility curves and are interpreted as an indication of the crossover from the paramagnetic (PM) to the SRO region. First- and second-order phase transitions are represented by red and blue lines, respectively. At temperatures below those delineated by blue lines different long-range order phases are stabilized. For fields above 8 T at low temperatures, a fully polarized (FP) state is formed. (b) Triangular magnetic lattice formed by Cu spins (Cu^{2+} ions) displayed as small blue spheres with exchange couplings of $J = 0.375$ meV along solid lines and $J' = 0.125$ meV along dashed lines. Our NMR measurements discussed in this paper were carried out on the Cs(A) site depicted by red spheres.

specific predictions of nonzero temperature properties are available. We consider two different spin liquid states, with elementary excitations that obey either bosonic or fermionic statistics, proposed earlier to describe the spin-1/2 Heisenberg AF on anisotropic triangular lattices. The bosonic Sp(N) large-N mean-field theory supports bosonic spinons that generically have a gap in the excitation spectrum [6, 17, 18]. By contrast, another family of mean-field theories supports fermionic spinons with no gap in the excitation spectrum [6, 7, 19, 20]. In the context of those theories (which assume non-interacting spinons), one can ask which description (bosons or fermions) yields a better mean-field description. Those two models have different temperature dependences of the nuclear magnetic resonance (NMR) relaxation rate, which we probe directly in the experiments.

Here we measure the local magnetization and the NMR relaxation rate to probe the magnetic behavior across the full phase diagram in the applied field, including the magnetically ordered phase at low temperatures, the SRO region above T_N and the high-temperature PM region. We focus on the properties in the SRO region of the phase diagram where spins are strongly correlated, but not on the long-range-ordered (LRO) region. By considering the temperature and field dependences of the rate, we deduce that the low-energy excitations in the SRO region are best characterized as gapless fermionic excitations. Furthermore, we compare our results with previous data on 1D chain materials [21, 22] and available theoretical models. The quasi-1D picture proposed in [11], which includes the effects of the strong but

frustrated interchain couplings in a consistent way, has not yet been extended to cover the intermediate temperature and field range. As most of our data were collected in this intermediate temperature and field range, we compare the results with alternative models of spin liquid phases for the anisotropic triangular lattice AF with fermionic excitations. Comparison of the NMR data to mean-field descriptions based on variational calculations using Gutzwiller-projected wavefunctions implies that in Cs_2CuCl_4 in the SRO region (at nonzero temperature and applied field) 2D interactions are important for a quantitative understanding of the low-energy properties. The rest of this paper is organized as follows. In section 2, the technical details of the NMR experimental setup are described. In section 3, we present the results for the temperature and magnetic field dependence of the NMR line and a comparison with experiments on 1D materials and with theoretical models. Finally, the conclusions are summarized in section 4.

2. Experiment

We used solution-grown single crystals of Cs_2CuCl_4. The measurements were carried out at the National High Magnetic Field Laboratory (NHMFL) using a 17 T sweepable magnet. We present data on one of the two magnetically inequivalent Cs sites, labeled Cs(A) and believed to be a better probe of the magnetism of Cu^{2+} ions due to its stronger hyperfine coupling [23]. At low temperatures ($T \lesssim 20$ K) quadrupolar effects on ^{133}Cs ($I = 7/2$) NMR are masked by the dominant magnetic broadening [23]. The NMR relaxation rate (T_1^{-1}) was measured as described in detail in [23]. In essence, the magnetization was saturated by applying a train of pulses equally spaced by a time $t < T_2$ at different frequencies across the magnetically broadened line. Following the saturation pulse train, the signal was detected after a variable delay time using a standard spin-echo sequence ($\pi/2$–τ–π). The Knight shift $K \equiv (\omega_N - H\gamma)/H\gamma$ is obtained from the frequency of the first spectral moment ω_N using the gyromagnetic ratio $^{133}\gamma = 5.5844\,\mathrm{MHz\,T^{-1}}$. The shift also provides a direct measure of the local magnetization $m_{\mathrm{loc}} = \mathbf{K}\cdot\mathbf{H}/A_{zz}$, since they are linearly related via the strength of the transferred hyperfine tensor (A_{zz}) [24]. For $\mathbf{H} \| \hat{c}$, the relevant component of the hyperfine tensor (A_{cc}) for determining m_{loc} is equal to $1.23\,\mathrm{T}\,\mu_{\mathrm{B}}^{-1}$ [24]. The only nonzero off-diagonal element of this symmetric hyperfine tensor is $A_{\mathrm{ac}} = \pm 0.185\,\mathrm{T}\,\mu_B^{-1}$ [24].

3. Results and discussion

Details of the temperature and applied field dependences of the NMR shift and rate are discussed to delineate different regions in the phase diagram of this frustrated magnetic system. Notably, we identify the temperature and applied field region where a state characterized by short-range antiferromagnetic correlations is stabilized, and we find good agreement with the results from bulk magnetization [15] and neutron scattering experiments [4]. Although this region cannot be distinguished from the PM one by any change of symmetry, it is appropriate to refer to it as SRO because spins are strongly correlated but not in an LRO state. We now discuss some further ways that our experiment distinguishes between the SRO and PM regions.

3.1. Temperature dependence

The temperature dependence of the shift at different H is illustrated in figure 2. It exhibits features typical of magnetization of any low-dimensional AF with short-range order. That is,

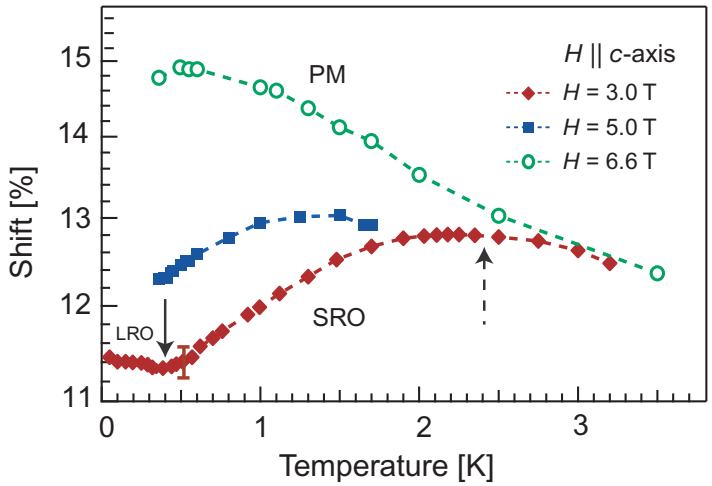

Figure 2. The T dependence of the NMR shift at different values of **H** applied along the $\hat{c}$-axis as denoted. A typical error bar is shown. The solid arrow denotes the transition between LRO and SRO. The dashed arrow denotes crossover between the SRO and PM regions.

in the SRO region the shift increases with increasing T, as is evident in the $H = 3\,\mathrm{T}$ data. This is in contrast to the shift in the PM state that decreases with increasing T, as is apparent from the $H = 6.6\,\mathrm{T}$ data. Thus, the characteristic T dependence delineates the boundary to the SRO region. The maximum in the temperature dependence of the shift signals a crossover from PM to SRO in the vicinity of $T \approx 2.4\,\mathrm{K}$. This finding is consistent with that from bulk magnetization measurements [15]. That is, the low field susceptibility, $\chi(T) = M/H$, displays a broad maximum at $T \approx 2.8\,\mathrm{K}$ characteristic of short-range antiferromagnetic correlations [15]. Moreover, the overall temperature dependence in zero field is described well by high-T series expansion models for the partially frustrated triangular lattice with $J = 4.46\,\mathrm{K}$ and $J'/J = 1/3$ [15].

The temperature dependence of the NMR relaxation rate also serves to distinguish each region of the phase diagram, as shown in figure 3. In the PM region, the rate increases as T is lowered. The rate reaches its maximum near $T \approx 2.4\,\mathrm{K}$ at $H = 3\,\mathrm{T}$, as is evident from the inset of figure 3. The maximum in T_1^{-1}, like the maximum in the T dependence of the shift, also indicates a crossover from PM to SRO. On further lowering the temperature in the SRO region, the relaxation rate decreases linearly with temperature. Below 500 mK the rate increases due to an enhancement of fluctuations associated with the transition to the LRO magnetic state. The exponential decrease of the rate below $T \approx 320\,\mathrm{mK}$ may be due to the opening of a spin gap in the LRO state (at $H = 3\,\mathrm{T}$).

3.2. Field dependence

The applied field dependence of the full-width at half-maximum (FWHM) of spectra at $T \approx 495\,\mathrm{mK}$ is plotted in figure 4. A typical spectrum, from which FWHM data were extracted, is shown in the inset of figure 4. At $T \approx 495\,\mathrm{mK}$ for fields below $\approx 7\,\mathrm{T}$ the system is in the SRO region, as discussed above. The FWHM smoothly increases with increasing H up to $\approx 7\,\mathrm{T}$. As FWHM measures the variation of the electron spin operator projected along the direction of H,

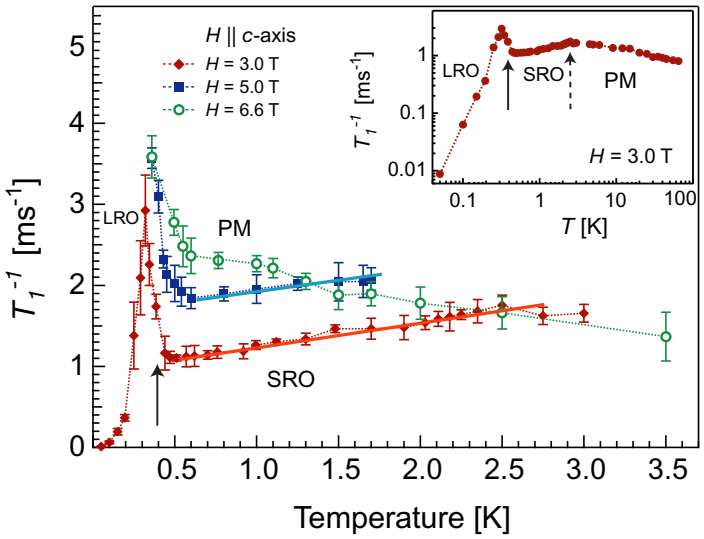

Figure 3. T_1^{-1} as a function of T for different values of **H** applied along the $\hat{c}$-axis. Solid lines denote linear T dependence. Inset: log–log plot of the T_1^{-1} versus T at $H = 3\,\mathrm{T}$. The solid arrow denotes the boundary between LRO and SRO. The dashed arrow denotes crossover between regions with different correlations.

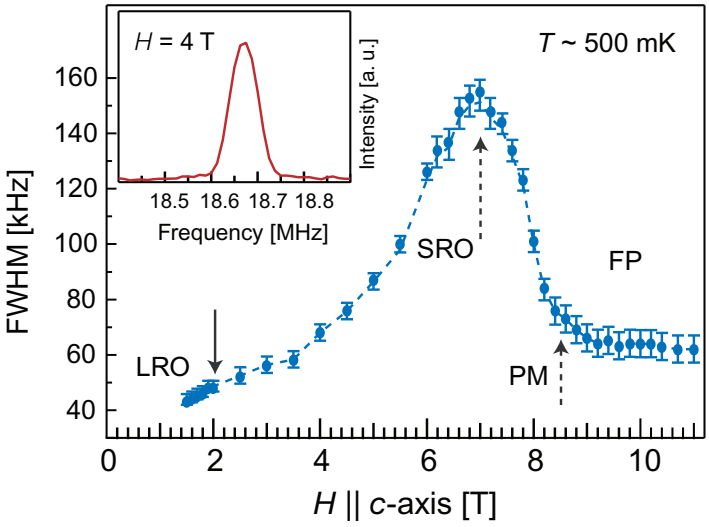

Figure 4. The applied field dependence of the FWHM of the NMR spectra. Inset: a representative ^{133}Cs NMR spectrum (at $T = 430\,\mathrm{mK}$ and $H = 4\,\mathrm{T}$) in the SRO region. The solid arrow denotes the boundary between LRO and SRO. The dashed arrows indicate crossovers from SRO to PM and then to FP.

the increase of FWHM implies increased static short-range correlation along the direction of $H \| c$ in the SRO region. We cannot exclude the possibility that some of the FWHM increase with H is due to a DM interaction. However, careful consideration of NMR spectra obtained when H is oriented away from the $\hat{c}$-axis led us to conclude that the contribution of DM interaction to FWHM is not a dominant one. For $7\,\mathrm{T} \lesssim H \lesssim 8.4\,\mathrm{T}$, the FWHM decreases with

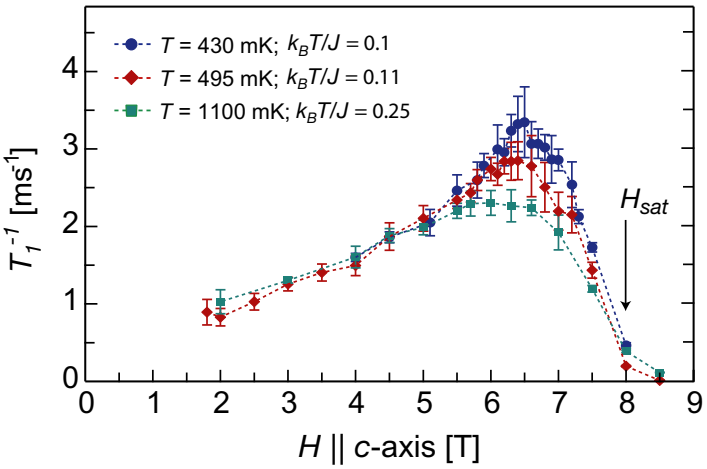

Figure 5. The NMR relaxation rate as a function of the H applied along the $\hat{c}$-axis at different temperatures.

increasing H as expected in the PM region, where static short-range correlations are suppressed. The field at which the FWHM reaches its maximum coincides with that where the maximum of the differential susceptibility ($\mathrm{d}m_{\mathrm{loc}}/\mathrm{d}H$) occurs [15]. Thus, the maximum in the FWHM indicates the onset of crossover from SRO to PM. In the FP state, the FWHM is constant as all spins are aligned with the field.

By examining the T and H dependences of the NMR observables, we are able to clearly identify the crossover from the SRO region. To gain further insight into the microscopic nature of this region, we proceed with the analysis of the H dependence of the relaxation rate. In figure 5, we plot the relaxation rate as a function of applied field. At low fields, as H increases, the rate rises steadily and attains its maximum at a field H_{M}. The maximum of the rate is smeared out by increasing temperature. At a given temperature, the maxima of both the rate and FWHM occur at nearly equal fields.

In the SRO region, the rate is T independent for H up to $\sim$5 T and, in the limit of $H \to 0$, it extrapolates to a nonzero value of $\sim$0.5 ms^{-1}. Furthermore, in the limit of $T \to 0$ the rate extrapolates to a nonzero value of $\sim$1 ms^{-1} at 3 T in the SRO region, as is evident from the data plotted in figure 3. The fact that the rate extrapolates to a nonzero value in the limit of $H \to 0$ and $T \to 0$ indicates that the rate is dominated by gapless excitations. Nonetheless, since the SRO region is stabilized at nonzero temperature we can only place an upper bound on the value of the gap (Δ) at $H = 0$. Specifically, the gap is smaller than the energy scale set by the smallest temperature ($T \simeq 430$ mK) probed in the SRO region in our experiment, $k_{\mathrm{B}}T \simeq 0.037$ meV $\approx J/10$. Strictly speaking, the evidence of gapless excitations clearly exists only for fields above 1.7 T (for technical reasons this was the lowest field probed in our experiment). For one Bohr magneton (Cu^{2+}, $S = 1/2$) a field of 1 T corresponds to $\simeq 0.06$ meV $\approx J/6$, which is of the same order of magnitude as the energy scale of some of the magnetic couplings in Cs_2CuCl_4. It is indeed possible that applying fields larger than 1 T might close a low-energy gap due to these weak couplings. However, as we will discuss in the next section, our data agree qualitatively with an observed evolution well described by gapless 1D fermionic excitations. Thus, we do not expect additional low-energy gaps to open up below 1 T, and even if that is the case, such a gap does not dominate the nature of the quasi-particles

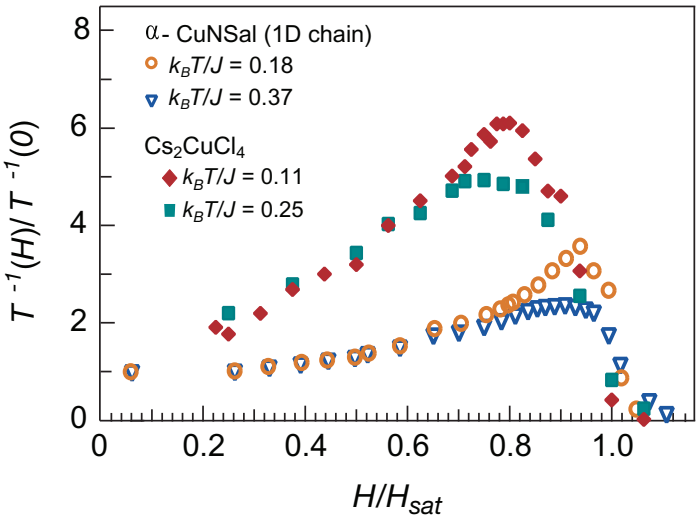

Figure 6. The magnetic field dependence of the NMR relaxation rates measured in Cs_2CuCl_4 and in the 1D spin-1/2 AF chain, α-CuNSal [21, 22].

over the wide field range of the SRO region. This suggests that the observed behavior of the rate in the SRO is dominated by gapless or nearly gapless excitations.

Although the spin dynamics above the ordering temperature is commonly governed by gapless critical fluctuations, the issue of the existence of a gap in this compound is nontrivial given the fact that the dominant excitations at base temperature occur in a dispersive continuum of excited states manifested at intermediate and high energies, which remains largely unchanged upon crossing the temperature-driven transitions from the ordered to the SRO region [4, 5]. Moreover, since neutron scattering experiments were not able to determine a tight bound on the gap, it is important to attempt to determine its value with a low-energy probe such as NMR, as in this work [4–6].

Having established that the excitations in the SRO region are gapless or nearly gapless, we proceed to examine the statistics of the excitations. The temperature dependence of the NMR rate is particularly sensitive to the statistics of the excitations [22, 25]. Assuming that the excitations are weakly interacting, the question is: which statistics (bosonic or fermionic) yields a better mean-field description of the temperature dependence of the rate? The absence of T dependence of the rate for H up to $\sim$5 T and the fact that the rate extrapolates to a nonzero value in the limit of $H \to 0$ and $T \to 0$ imply that gapless excitations are fermionic [21]. By contrast, bosonic excitations would lead to a much stronger dependence on temperature [8, 21, 25], in disagreement with the data. As discussed in the introduction, the gapless excitations are predicted by fermionic treatments. A similarly small value of the gap can be obtained from a bosonic treatment if the system is close to a second-order phase transition [6]; however, fermionic spin liquids offer a more natural explanation of the data.

3.3. Comparison with the 1D spin chain

The observed field and temperature dependence of the relaxation rate resembles that measured in the 1D spin-1/2 AF chain compound α-CuNSal, as illustrated in figure 6 [21, 25]. For $H < H_{sat}$, our data agree qualitatively with an observed evolution well described by gapless 1D fermionic

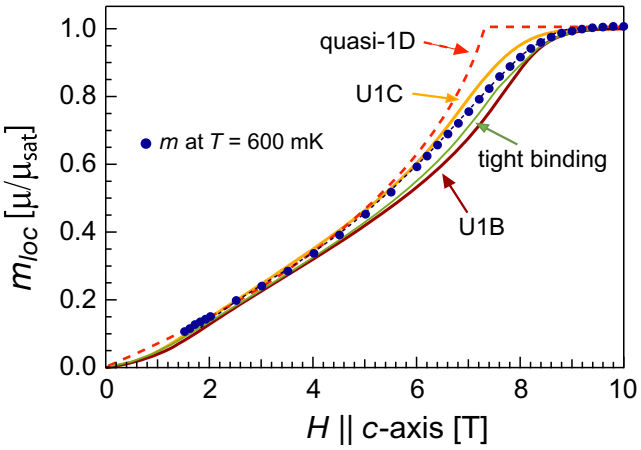

Figure 7. Dependence of magnetization on applied field as calculated at $T = 600\,\mathrm{mK}$ in the two different U(1) spin-liquid models (see text) and, for purposes of comparison, a tight-binding model on the anisotropic triangular lattice and a quasi-1D model at zero temperature described in [10] for $J = 0.374\,\mathrm{meV}$ and $J' = 0.128\,\mathrm{meV}$. The calculated magnetization is compared to experimental measurements. In the PM regime $7\,\mathrm{T} \lesssim H \lesssim 8\,\mathrm{T}$, the mean-field theory does not apply and consequently a comparison of measurements and calculations is not meaningful.

excitations [21, 22], suggesting that the rate in Cs_2CuCl_4 may be dominated by conventional spinons found in 1D. On the other hand, there are significant quantitative differences, indicating that the strong interchain interactions produce measurable effects. In particular, the peak in the rate at H is found significantly lower than at H_{sat}, and at low fields the data display a stronger dependence on the field than expected from the model. Furthermore, for comparable values of $k_{\mathrm{B}}T/J$ both the measured and calculated 1D rates [21, 22] exhibit a sharper peak than that evident in the Cs_2CuCl_4 data.

In figure 7, we show a comparison of the magnetization data with the zero-temperature quasi-1D model proposed by Starykh and Balents [10]. This treats the 1D chain exactly and the interchain interaction J at mean-field level. Thus, if external field is H, then the effective field felt by spins on the 1D chain is slightly smaller, $H_{1d} = H - 4J' \cdot S_z$, where S_z is magnetization in field H_{1d}, $S_z = 1/\pi \arcsin(1/(1 - \pi/2 + \pi J/H_{1d}))$, $g = 2.3$, $J = 0.374\,\mathrm{meV}$, $J' = 0.128\,\mathrm{meV}$ and $S_z = 1/2$ at $H_{1d} = 2J$. The disagreement between the data and the quasi-1D model appears at high fields near saturation as the quasi-1D model predicts saturation at a field $2J + 2J'$ and not at $2J + 2J' + J'^2/2J$, as follows from the spin-wave theory [15, 26]. Furthermore, effects of the interlayer and DM interaction are not included in the quasi-1D model, nor is rounding due to nonzero temperature ($k_{\mathrm{B}}T/J = 0.14$). For completeness, in the section below we also compare the data with alternative models of spin liquids relevant for the anisotropic triangular-lattice AF, where the effects of temperature can be treated explicitly.

3.4. 2D spin-liquid models

For the triangular lattice AF, a number of spin-liquid states have been theoretically proposed based on symmetry arguments [7]. Relevant to the anisotropic triangular lattice and possessing

gapless fermionic spinons are two $U(1)$ spin liquids, one with commensurate SRO (U1B) and one with incommensurate SRO (U1C). A variational study of related states is described in [9]. Here, we compare the results of static (magnetization) and dynamic (relaxation rate) measurements to predictions based on a combination of Gutzwiller-projected wavefunctions and mean-field theory. Parameters of the mean-field theory are chosen to minimize the ground state energy of the corresponding Gutzwiller-projected wavefunctions. For simplicity, the parameters are optimized for the case of zero applied magnetic field and then kept constant over the entire phase diagram. For $J/J' \approx 3$, the optimized parameters exhibit an enhanced 1D character as the ratio of intra-chain to inter-chain hopping amplitudes is $\lambda/\chi = 7$ and $\lambda/\chi = 8$ for the U1B and U1C states, respectively. The enhancement of 1D correlations is broadly consistent with the quasi-1D picture of Kohno *et al* [11].

At the mean-field level, the spinons are non-interacting and the magnetic field acts via Zeeman coupling as a chemical potential of opposite sign for spin-up and -down spinons, changing their relative populations. We set the bandwidth of the spinon dispersion so that the critical field required for full polarization of the spins matches that of the experiment in the limit of $T \to 0$. A comparison between the calculated magnetization in the different spin liquid states, as well as for an anisotropic tight-binding model, and the experimentally measured values is shown in figure 7. Similar to the quasi-1D model, both 2D models give a good qualitative description of the data, and the U1C model fits best quantitatively for $H \lesssim 7\,\mathrm{T}$. For $7\,\mathrm{T} \lesssim H \lesssim 8\,\mathrm{T}$, the comparison is not meaningful because there is a crossover from the SRO to PM regime at $\approx$7 T prior to full polarization at $\approx$8 T. The PM state is captured neither by mean-field theory nor by the tight-binding model because the bonds have been held constant at their zero temperature values. In addition, the slight disagreement between calculations and data near saturation may also be due to the small inter-layer coupling and DM interaction, both of the order of $\sim$5% J, which are not included in the theoretical model and assumed to lead only to a small upward rescaling of the saturation field.

The relaxation rate for a field oriented along the z-direction is given by [27]

$$\frac{1}{T_{1z}} = \frac{(\gamma_{Cs}\mu_B)^2}{\hbar^2} \sum_{\beta=x,y} \sum_{i,j} (A_{i,x\beta}A^*_{j,x\beta} + A_{i,y\beta}A^*_{j,y\beta}) \mathrm{Re} \int_0^\infty \mathrm{d}t \exp(\mathrm{i}\,\omega t) \langle\{\delta S_{i\beta}(t),\ \delta S_{j\beta}(0)\}\rangle, \quad (1)$$

where $A_{i,\alpha\beta}$ denote components of the hyperfine coupling tensor at site i and $\delta\mathbf{S}_i = \mathbf{S}_i - \langle\mathbf{S}_i\rangle$. Since the ^{133}Cs(A) ions are located close to the center of a triangle of Cu^{2+} spins [24], momentum-dependent form factors are important and have been included in the calculation. With the assumption that the Cs(A) ions are located at the center of the triangle, the form factor reduces to $|A(\mathbf{q})|^2 = A^2(3 + 2\cos(q_x) + 2\cos(q_y) + 2\cos(q_x - q_y))$.[6] However, the most important term in the sum in equation (1) is due to the transverse ($\beta = x, y$) autocorrelation function ($i = j$), which gives the following approximate form:

$$\frac{1}{T_{1z}} \propto \int_{-\infty}^{\infty} \mathrm{d}\mathcal{E} \frac{\mathrm{d}f(\mathcal{E})}{\mathrm{d}\mathcal{E}}\Big|_{\mathcal{E}=\mu} \mathcal{N}(\mathcal{E})\mathcal{N}(\mathcal{E} - 2\mu), \quad (2)$$

where $f(\mathcal{E})$ is the Fermi–Dirac distribution, $\mathcal{N}$ the density of states (DOS) and μ is the Zeeman-shifted chemical potential. The dominant contribution to the correlation function is proportional to the product of two Fermi functions and is the result of scattering two spin-1/2 spinons.

[6] The NMR rate is dominated by the fluctuations that couple via the diagonal component of the hyperfine tensor. Thus, the off-diagonal components of the hyperfine tensor A_{ac} and A_{ca}, crucial for understanding the details of the NMR lineshape (more so in the LRO phases), are less important for determining the NMR rate.

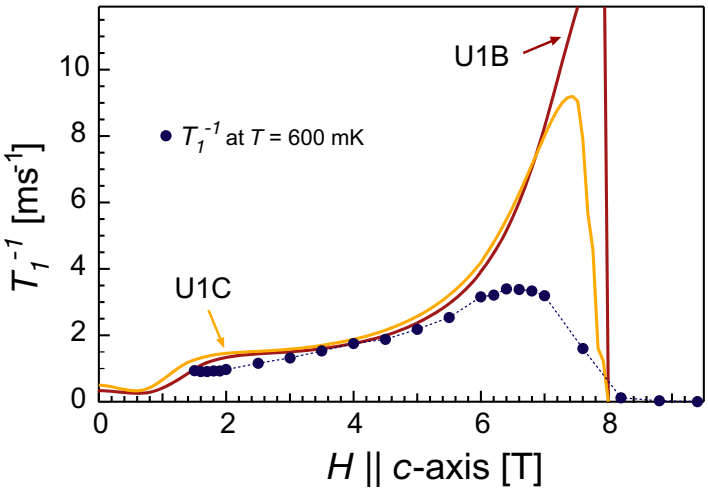

Figure 8. Calculated field evolution of the NMR relaxation rate for the two different U(1) spin liquid models at $T = 600\,\mathrm{mK}$ using equation (1). Dark blue symbols are the data. The dotted curve is a guide to the eye.

The relaxation rate of the two $U(1)$ SL states is plotted in figure 8. As is evident from equation (2), peaks in the relaxation rate correspond to maxima in the DOS. For the U1C state, the peak occurs prior to saturation at $H \approx 0.9H_{\mathrm{sat}}$, closer to the observed value of $H \approx 0.8H_{\mathrm{sat}}$. This is because for U1C DOS is a maximum before saturation is reached, whereas for U1B the peak is at H_{sat}. Unlike the U1B phase, the DOS for the U1C phase reaches a constant value at the top and bottom of the bands at saturation. In contrast, the rate vanishes at low fields in the $T \to 0$ limit in both states because the DOS vanishes at the Fermi surface. As calculations are performed at a nonzero temperature of 600 mK, the rate reaches a nonzero value at zero field. Both models agree with data at intermediate fields but not near saturation, where data show no evidence for a sharp peak/divergence. This may be due to oversimplification in the mean-field approximation for the theoretical models, or the fact that the mean-field parameters are optimized for zero field (see above) so that the high-field behavior can be not more than qualitatively correct.

Important quantitative and qualitative differences between the calculated and the experimentally measured rates remain. The derivative of $f(\mathcal{E})$ in equation (2) leads to a stronger temperature dependence of the relaxation rate than evidenced experimentally in figure 3. In particular, the rate as calculated in the mean-field approximation vanishes at zero temperature. By contrast, an extrapolation of the T_1^{-1} SL data plotted in figure 3 down to zero temperature yields $T_1^{-1} \approx 1\,\mathrm{ms}^{-1}$ at $H = 3\,\mathrm{T}$. The discrepancy may stem from the fact that the calculated rate, unlike the (one-point) magnetization, is affected by correlations neglected in the mean-field approximation [10]. Gutzwiller projection is known to change the power-law exponent of the algebraically decaying spin–spin correlations in SL phases [28]. In 1D, where the rate can be calculated using a Jordan–Wigner transformation to represent spin excitations as spinless fermions, there is only a weak dependence on temperature [22]. Thus, the observed weak dependence of the relaxation rate on temperature may also point to the dynamics in the SRO state of Cs_2CuCl_4 being more like that of 1D spinons traveling along individual chains [11].

4. Conclusions

We have probed the low-energy excitations in the spin-1/2 anisotropic triangular AF Cs_2CuCl_4. We found that the SRO region stabilized at intermediate temperatures and applied fields is best characterized by gapless or nearly gapless fermionic spinon excitations, with experiments yielding an upper bound on the size of the gap value of $0.037\,\text{meV} \approx J/10$. We compared the observed field dependence of the magnetization and NMR rate with mean-field theories proposed for anisotropic triangular lattice AF and found good quantitative agreement for the field dependence of the NMR relaxation rate at intermediate fields. Our results call for an extension of the self-consistent quasi-1D picture [11] and other theoretical models for spin liquid states in the anisotropic triangular lattice quantum AF to include quantitative predictions for the field and temperature dependence of the NMR relaxation rate.

Acknowledgments

We thank L Engel, T Murphey and E Palm for help with the experiments. This work was supported in part by the NSF (DMR-0547938 and DMR-0605619). A portion of this study was performed at the NHMFL, which is supported by NSF Cooperative Agreement no. DMR-0084173, by the State of Florida and by the DOE. VFM acknowledges support from the A P Sloan Foundation.

References

[1] Fadeev L D and Takhtajan L A 1981 *Phys. Lett.* A **85** 375
[2] Haldane F D M and Zirnbauer M R 1993 *Phys. Rev. Lett.* **71** 4055
[3] Tennant D A, Cowley R A, Nagler S E and Tsvelik A M 1995 *Phys. Rev.* B **52** 13368
[4] Coldea R, Tennant D A, Tsvelik A M and Tylczynski Z 2001 *Phys. Rev. Lett.* **86** 1335
[5] Coldea R, Tennant D A and Tylczynski Z 2003 *Phys. Rev.* B **68** 134424
[6] Chung C H, Marston J B and McKenzie R H 2001 *J. Phys.: Condens. Matter* **13** 5159
[7] Zhou Y and Wen X-G 2003 arXiv:cond-mat/0210662
[8] Chung C-H, Voelker K and Kim Y B 2003 *Phys. Rev.* B **68** 094412
[9] Yunoki S and Sorella S 2006 *Phys. Rev.* B **74** 014408
[10] Starykh O A and Balents L 2007 *Phys. Rev. Lett.* **98** 077205
[11] Kohno M, Starykh O A and Balents L 2007 *Nat. Phys.* **3** 790
[12] Kohno M 2009 *Phys. Rev. Lett.* **103** 197203
[13] Coldea R, Tennant D A, Cowley R A, McMorrow D F, Dorner B and Tylczynski Z 1996 *J. Phys.: Condens. Matter* **8** 7473
[14] Coldea R, Tennant D A, Habicht K, Smeibidl P, Wolters C and Tylczynski Z 2002 *Phys. Rev. Lett.* **88** 137203
[15] Tokiwa Y, Radu T, Coldea R, Wilhelm H, Tylczynski Z and Steglich F 2006 *Phys. Rev.* B **73** 134414
[16] Coldea R 2009 private communication
[17] Read N and Sachdev S 1991 *Phys. Rev. Lett.* **66** 1773
[18] Sachdev S 1992 *Phys. Rev.* B **45** 12377
Sachdev S and Read N 1991 *Int. J. Mod. Phys.* B **5** 219
[19] Affleck I and Marston J B 1988 *Phys. Rev.* B **37** 3774
Affleck I *et al* 1988 *Phys. Rev.* B **38** 745
Dagotto E, Fradkin E and Moreo A 1988 *Phys. Rev.* B **38** 2926
[20] Wen X-G 2002 *Phys. Rev.* B **65** 165113

[21] Azevedo L J, Narath A, Richards P M and Soos Z G 1979 *Phys. Rev. Lett.* **43** 875
[22] Azevedo L J, Narath A, Richards P M and Soos Z G 1980 *Phys. Rev.* B **21** 2871
[23] Vachon M-A, Kundhikanjana W, Straub A, Mitrović V F, Reyes A P, Kuhns P, Coldea R and Tylczynski Z 2006 *New J. Phys.* **8** 222
[24] Vachon M-A, Koutroulakis G, Mitrović V F, Reyes A P, Kuhns P, Coldea R and Tylczynski Z 2008 *J. Phys.: Condens. Matter* **20** 295225
[25] Ehrenfreund E, Rybaczewski E F, Garito A F, Heeger A J and Pincus P 1973 *Phys. Rev.* B **7** 421
[26] Veillette M Y, Chalker J T and Coldea R 2005 *Phys. Rev.* B **71** 214426
[27] Moriya T 1962 *Prog. Theor. Phys.* **16** 23
[28] Paramekanti A and Marston J B 2007 *J. Phys.: Condens. Matter* **19** 125215